DYNAMICAL RESPONSES TO DIURNAL HEATING IN TROPICAL CYCLONES AS SEEN IN A LINEAR MODEL

Rebecca C. Evans* and David S. Nolan

University of Miami, Miami, Florida

1 INTRODUCTION

The diurnal cycle (DC) in radiation has long been known to manifest itself in the cirrus canopy of tropical cyclones (TCs), such as in its radial extent, and diurnal pulses of convection (Kossin 2002; Dunion et al. 2014). Dunion et al. (2014), showed that for all major North Atlantic hurricanes from 2001-2010, a peak in IR Brightness Temperature forms in the inner core of the cyclone around the time of local sunset and propagates radially outwards overnight. This signal likely forms due to radiative cooling of the cloud tops generating convection. Alternately this may form due to differential cooling of clouds and the surrounding cloud-free regions, or radiative cooling altering the potential vorticity of the cirrus canopy (Gray and Jacobson 1977; Mecikalski and Tripoli 1998). Regardless of the mechanism by which the pulse radiates, behind this feature there is a marked warming, leading to structural and perhaps intensity changes (Dunion et al. 2014). Furthermore, the DC has been shown to be important for regulating tropical cyclogenesis and secondary eyewall formation, since solar heating enhances the moat between eyewalls, and night is necessary for allowing the reestablishment of moisture removed by heating during the day (Tang and Zhang 2016; Tang et al. 2017).

Other studies on the diurnal cycle have focused on the transition between balanced and radiating waves in response to diurnal heating (Willoughby 2009; Navarro and Hakim 2016; Navarro et al. 2017; O'Neill et al. 2017). Willoughby (2009) used an idealized framework to evaluate secondary circulations produced in response to forcing with low periods. Navarro and Hakim (2016) and Navarro et al. (2017) used an idealized model with full physics, treating diurnal forcing as a sine wave, to find that diurnal forcing of the cirrus canopy results in a diurnal cycle of storm intensity. O'Neill et al. (2017) explored the transition between balanced and radiating waves with periods of 12 hours or longer. They found that diurnal heating of the cirrus canopy creates a balanced response in the inner core, and radiating waves in the storm environment, with responses predominantly of diurnal and semi-diurnal periods. The internal inertia gravity waves (IIGWs) created were not observed in the inner core because inside the region of moist convection, the horizontal extent of instability release is small. Outside the inner core remains statically stable, supporting IIGWs.

The question remains, where does the diurnal pulse in the cirrus canopy as shown by Dunion et al. (2014) originate? In particular, does it originate from diurnal forcing of convection in the eyewall or from the cirrus canopy itself? Furthermore, where do diurnal signals outside the inner core originate? In this study, we aim to use a linear model to investigate balanced vs. radiating responses to diurnal heating of the cirrus canopy and eyewall in TCs.

* *Corresponding Author Address:* Rebecca C. Evans, University of Miami, Rosenstiel School of Marine and Atmospheric Science, 4600 Rickenbacker Causeway, Miami, FL, 33149; email: rebecca.evans@rsmas.miami.edu

2 METHODOLOGY

2.1 3DVPAS Description

This study evaluates the dynamical responses to potential temperature forcing in the eyewall and cirrus canopy of a dry hurricane-like axisymmetric vortex. The model, the **3**-**D**imensional **V**ortex **P**erturbation **A**nalysis and **S**imulation (3DVPAS), is based upon the vortex anelastic equations as derived in Hodyss and Nolan (2007) and Nolan et al. (2007). The model simulates the evolution of free or forced perturbations to a balanced vortex.

The domain for the simulations is cylindrical with solid boundaries, extending to a radius of 800km, and height of 20km. At the upper and outer boundaries, there are Gaussian damping zones to absorb waves. Simulations were performed with a horizontal resolution of 5km and vertical resolution of 0.6km. The basic state for the simulations is a Modified Rankine Vortex, assuming slantwise moist neutral conditions in gradient wind balance as shown in Figure 1.

3DVPAS was forced using potential temperature perturbations $(\theta'(r,z,t))$ where r is radius, z is height, and t is time. The shape of the θ' forcing in r-z space and the temporal forcing were idealized versions of the diabatic heating analyzed in the Hurricane Nature Run (Nolan et al. 2013).

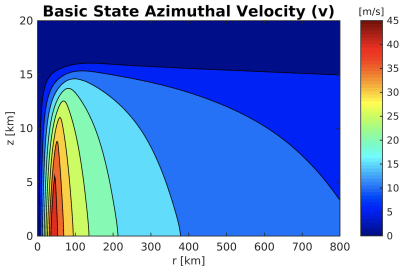

Figure 1: Basic state azimuthal velocity, $\bar{v}$, with an outward slope of radius of maximum winds (RMW). The surface wind maximum of 45m/s, is located at a radius of 40km.

2.2 Hurricane Nature Run (HNR)

2.2.1 Description

The Nolan et al. (2013) Hurricane Nature Run (HNR) is a simulation of the life cycle of a strong tropical cyclone in the North Atlantic Ocean using the Weather Research and Forecasting Model version 3.2.1 (WRF), embedded in the Joint Observing System Simulation Experiment (OSSE) global nature run by the European Center for Medium-Range Weather Forecasts (ECMWF). The resolution of the innermost nest is 1km. Solar radiation was parameterized using the RRTM-G scheme (Iacono et al. 2008). Azimuthally averaged fields of diabatic heating will be used here to determine the spatial structure and temporal variability of diurnal heating in the HNR.

2.2.2 Spatial variability of heating

The spatial structure of radiative heating at the time of the daily minimum (0600z) in the HNR is shown in Figure 2a, which illustrates the two main cloud bodies with strong diurnal variability in radiative heating: the cirrus canopy and the eyewall. The eyewall heating is displaced around 10km inwards of the radius of maximum wind (RMW), and extends from around 2-10km height.

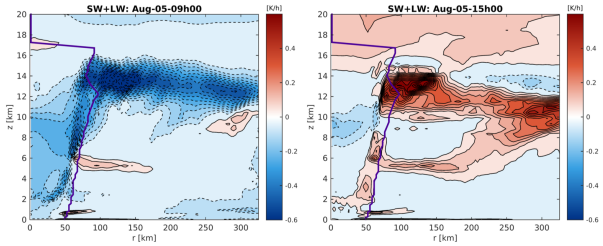

(a) Minimum: 0900z *(b) Maximum: 1500z*

Figure 2: Radius-height plots of the (a) minimum (0900z) and (b) maximum net radiative heating (shortwave plus longwave) (1500z). Note also the consistent positive radiative heating at the melting level, due to continuous heating from longwave radiation emitted below. Mean position of the RMW is shown by the purple line.

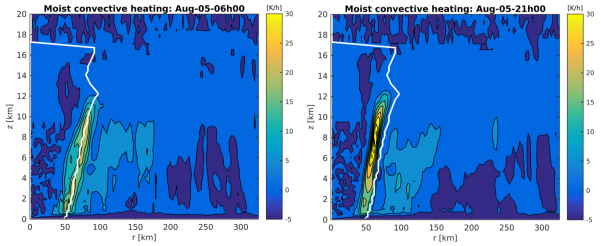

(a) Minimum: 0600z *(b) Maximum: 2100z*

Figure 3: Radius-height plots of the (a) minimum (0600z) and (b) maximum (2100z) moist convective heating (latent heating). Note the only location of significant moist convective heating is the eyewall. Mean position of the RMW is shown by the white line.

At the daily maximum of radiative heating (1500z), in Figure 2b, it is shown that cirrus clouds and the thick clouds at the top of the eyewall absorb most to the incoming shortwave radiation atop the cyclone, preventing solar heating of the clouds below. Thus diurnal variability of radiative heating is greatest in the cirrus canopy where the clouds are most susceptible to solar heating.

As shown in Figure 3, moist convective heating dominates in the eyewall. This is weakest at 0600z as shown in Figure 3a, and strongest at local sunset at 2100z, as in Figure 3b. The heating rates due to moist convection are substantially greater than for radiative heating.

2.2.3 Temporal variability of heating

To determine the variability in heating rates throughout the course of one day, time series of the area-averaged heating in the cirrus canopy and eyewall were constructed. The area averages for the eyewall were taken over a slanted box displaced inwards of the RMW, extending from z=2-10km and of width 10km. The center of the box was colocated with the maximum moist convective heating. The cirrus canopy area average was taken over a box from r=75-170km and z=12-14km. This aimed to capture diurnal variability at the location of the maximum of radiative heating. Using these time series, a daily composite was created for moist convective heating in the eyewall, radiative heating in the eyewall, and radiative heating in the cirrus canopy (Figure 4).

As shown in Figure 4, eyewall convection is strongest around local sunset (2100z), and weakest at 0600z. The diurnal heating rate is sinusoidal in shape. In the lower panel of Figure 4, eyewall radiative heating is shown to be consistently negative, since the thick clouds are largely opaque to solar shortwave heating while constantly emitting longwave radiation. The cirrus canopy is strongly heated during the day since it is located at the uppermost levels. The peak of this heating occurs at 1500-1600z, while the strongest cooling is from sunset after 2100z to sunrise at 0900z.

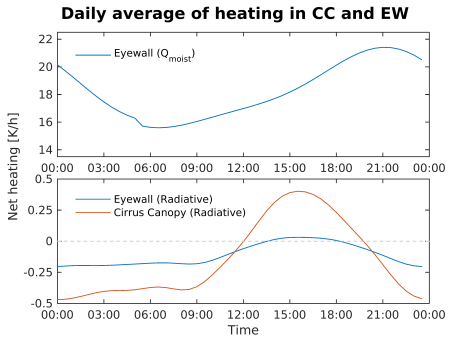

Figure 4: The diurnal cycle of (upper) moist convective heating and (lower) radiative heating for the cirrus canopy (CC) and eyewall (EW). Blue lines show the diurnal cycle for the eyewall, and the red line shows the diurnal cycle for the cirrus canopy.

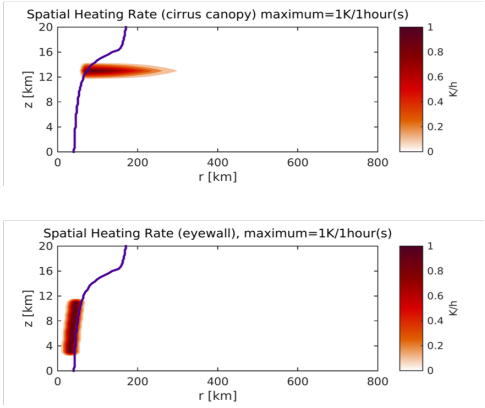

Figure 5: Idealized r-z structure of the θ' forcing used in 3DVPAS to represent the (a) CC and (b) EW. Deepest red colors indicate the maximum heating (θ'). The purple line is the RMW

2.3 Idealized 3DVPAS simulations

Using the spatial structure of radiative and moist convective heating from Figure 2 and Figure 3 as a guide, idealized potential temperature perturbations in the shape of the cirrus canopy and eyewall were designed for use as forcing in 3DVPAS (Figure 5). For the idealized cirrus canopy (hereafter referred to as CC), the perturbation potential temperature (θ') is maximized at the RMW at a height of 13km, and the CC extends to a radius of around 300km. The idealized eyewall (hereafter referred to as EW) is displaced 10km inwards of the RMW, and slopes outwards with height concurrently with the slope of the RMW. The model EW extends from 2km height to 11km.

The heating rate is forced to change in time for four model days using an idealized version of the daily heating rates shown in Figure 4. 3DVPAS simulates perturbations to the mean state, so the diurnal cycle for moist convective heating in the eyewall in the upper panel of Figure 4 was adjusted to have a mean of zero instead of 18K/h, but maintains the same amplitude of the forcing and timings of the maximum and minimum. The radiative heating cycle was also idealized for the CC and EW, again maintaining the amplitude and phase shown in Figure 4.

Based on the HNR, three simulations were performed in 3DVPAS to evaluate the transition between balanced and radiating responses produced by the diurnal forcing of (1) moist convective heating in the eyewall, (2) radiative heating in the eyewall, and (3) radiative heating in the cirrus canopy.

3 RESULTS

3.1 Moist convective heating in the eyewall

Figure 6 shows the progression of perturbation vertical motion, w', from the maximum of daily moist convective heating in the EW to the minimum.

At the maximum, in Figure 6a, during positive θ' in the EW there is strong upward motion throughout the entire EW, with compensating downward motion either side of the eyewall, downward motion in the region of the cirrus canopy, and downward motion at the edge of the domain, closing the circulation. During the transition from positive to negative heating rate, as in Figure 6b, w' declines fastest near the surface where the mean azimuthal wind, $\bar{v}$, is greater. w' at the top of the eyewall, where $\bar{v}$ is much lower, responds more slowly. At the minimum in eyewall moist convective heating, in Figure 6c, the spatial pattern is the exact opposite of that in Figure 6a since in a linear model the opposite sign of heating yields the opposite sign of motion.

All the panels in Figure 6 illustrate that the motion produced in response to heating from moist convection in the EW is entirely balanced, with no radiating response. This is due to the very high inertial stability in the EW, where $\bar{v}$ is highest, which prevents the radiation of waves produced by the low-frequency forcing. In a linear model, the spectrum of frequencies that makes up the temporal forcing function should also manifests themselves in the response. Since the temporal forcing function used in this simulation is a sinusoidal wave of exactly diurnal frequency, the frequency of the response is also entirely diurnal.

3.2 Radiative heating in the eyewall

Similarly to the EW moist convective heating in subsection 3.1, the response to diurnal radiative heating in the EW is also largely balanced as shown in Figure 7. The panels in Figure 7 show the progression of w' from model sunrise to sunset, with additional snapshots just after sunrise and during the peak radiative heating.

At sunrise, w' in Figure 7a looks much like that of the minimum in moist convective heating, i.e. the response at

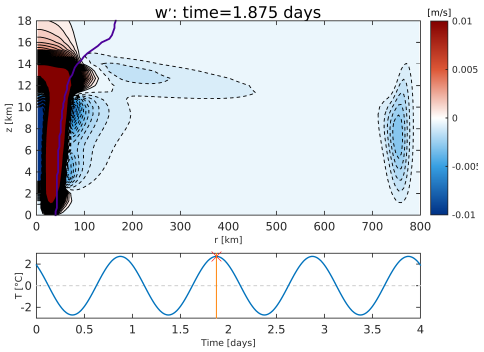

(a) w' at 1.875 days

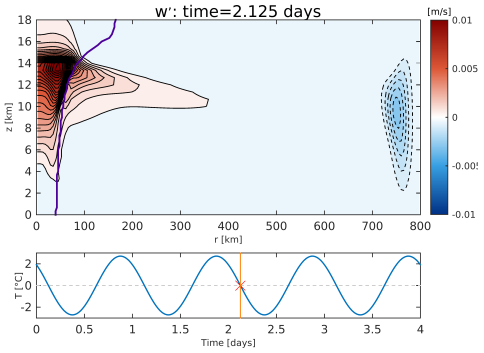

(b) w' at 2.125 days

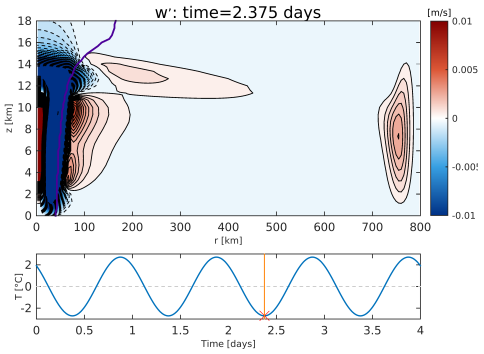

(c) w' at 2.375 days

Figure 6: Moist convective heating in the EW: r-z snapshots of w' at (a) 1.875 days, (b) 2.125 days, (c) 2.375 days. Red colors denote upward motion, and blue colors downward motion. The colorbar is saturated at 10% of maximum w' to observe finer details of waves. Below each r-z snapshot, the temporal forcing used in the simulation and the corresponding point in time at which the snapshot was taken are shown (denoted by the orange line and marker). The purple line is the RMW.

this time is balanced. Just after sunrise however, there is evidence of a radiating feature at a radius of 500km, and height of 6-8km (Figure 7b). This negative w' radiates outwards and downwards from the top of the EW, reaching the edge of the domain by the time of the peak radiative heating at 1.5 days in Figure 7c. The radiating wave is of extremely low amplitude (around -1x10^{-5}m/s). Otherwise the majority of the cyclone outside the RMW remains devoid of any w' throughout the simulation. By sunset, w' becomes almost entirely balanced again as evident in Figure 7d, closely resembling w' at sunrise.

As mentioned in subsection 3.1, any waves produced in response to heating have the same frequencies as the temporal heating rate function with which they were forced. The radiative heating forcing function has sharp inflection points at sunrise and sunset, and so projects on to modes of higher frequency that one cycle/day. Specifically, these modes have periods of even fractions of 24 hours (i.e. periods of 24, 12, 8, 6, and 4 hours). As such, waves produced in response to the radiative forcing have these same frequencies. The wave shown in Figure 7b and Figure 7c corresponds to these higher frequency waves produced by the relatively sudden change in heating rate.

As shown in Figure 7, while some of the higher frequency components of the response can radiate in to the outer cyclone, they are effectively negligible. Therefore, regardless of the shape of the temporal forcing function, heating in the EW produces a balanced response that is confined near to the source of the heating in the EW by the high inertial stability associated with the higher $\bar{v}$ and lower r.

3.3 Radiative heating in the cirrus canopy

For the diurnal radiative heating if the CC, the response to heating is essentially the opposite in character to that of the EW, in that it is almost entirely radiating. This is shown in Figure 8, which, as for the corresponding EW simulation, shows the progression of the w' field from sunrise to sunset.

At sunrise, in Figure 8a, the heating rate is negative, resulting in downward w' at the CC, and compensating upward motion in the eye and outer radii at upper levels. Waves produced by the downward motion in the CC radiate outwards and downwards. As with the EW, just after sunrise, in Figure 8b, the sudden change in heating rate induces the formation of waves of multiple frequencies. The waves of higher frequency can be seen in the figure to radiate at a steeper angle from the horizontal than the waves of lower frequencies. The variability in angle of radiation matches very well with the results of O'Neill et al. (2017) for internal inertia gravity waves radiating from the cirrus canopy in a full physics model. At the peak solar heating in Figure 8c the w' response is essentially the opposite of that at sunrise, with upward motion in the CC with compensating downward motion either side. By sunset in Figure 8d, there are fewer waves at the surface, since most of the waves have radiated vertically away from the surface by this time.

The forcing is situated at a high elevation where $\bar{v}$ is much lower than for the forcing in the EW simulations. Therefore, the inertial stability is significantly lower, allowing the horizontal radiation of waves. A significant amount of the diurnal signal of w' in the CC of TCs thus originates from diurnal forcing of the CC itself rather than the EW.

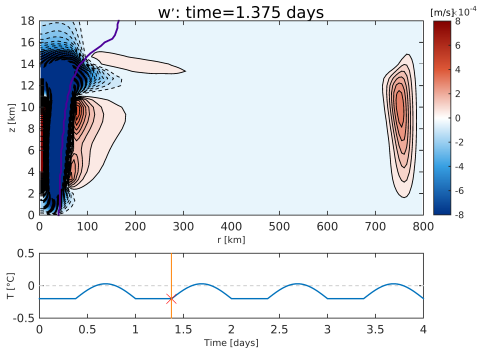

(a) w' at 1.375 days

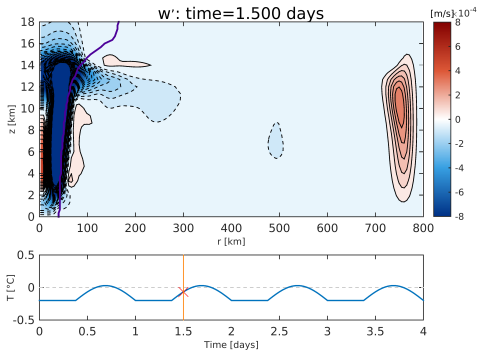

(b) w' at 1.500 days

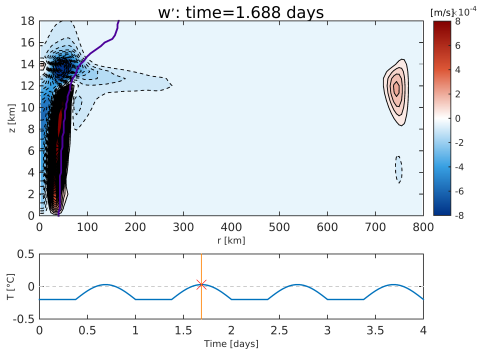

(c) w' at 1.688 days

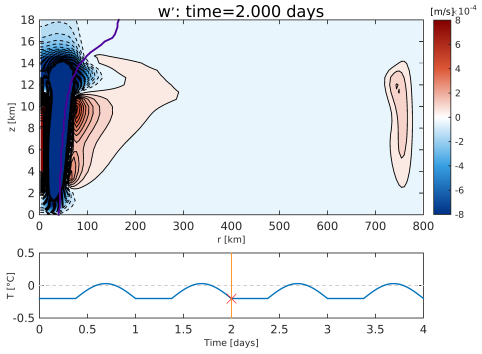

(d) w' at 2.000 days

Figure 7: Radiative heating in the EW: r-z snapshots of w' at (a) 1.375 days, (b) 1.500 days, (c) 1.688 days, (d) 2.000 days. The colorbar is saturated at 10% of maximum w' to observe finer details of waves. Below each r-z snapshot, the temporal forcing used in the simulation and the corresponding point in time at which the snapshot was taken are shown (denoted by the orange line and marker). The purple line is the RMW.

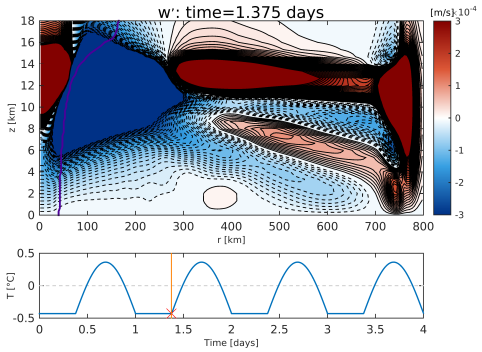

(a) w' at 1.375 days

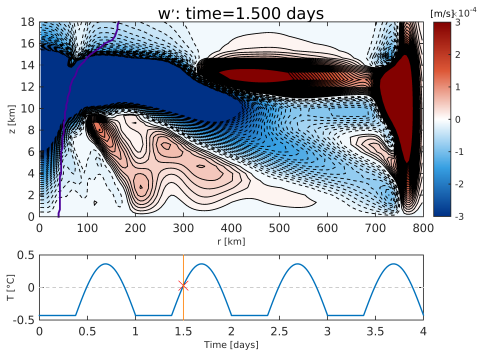

(b) w' at 1.500 days

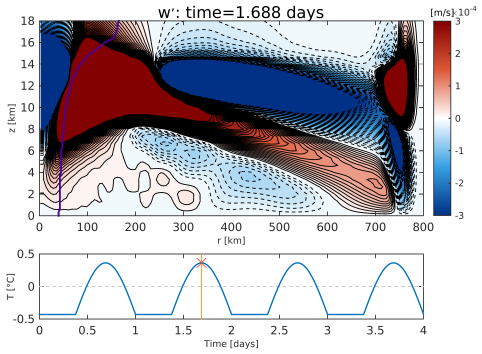

(c) w' at 1.688 days

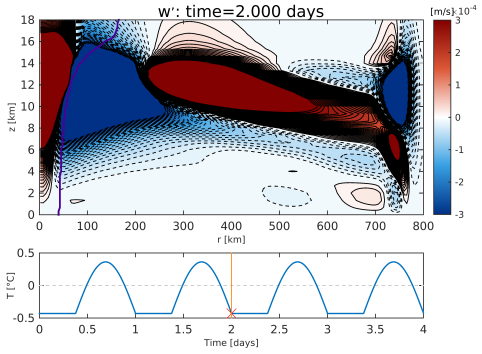

(d) w' at 2.000 days

Figure 8: Radiative heating in the CC: r-z snapshots of w' at (a) 1.375 days, (b) 1.500 days, (c) 1.688 days, (d) 2.000 days. The colorbar is saturated at 10% of maximum w' to observe finer details of waves. Below each r-z snapshot, the temporal forcing used in the simulation and the corresponding point in time at which the snapshot was taken are shown (denoted by the orange line and marker). The purple line is the RMW.

4 SUMMARY

The main sources of diurnal heating in a TC are moist convective heating of the eyewall, and radiative heating of the cirrus canopy and eyewall. Using the Nolan et al. (2013) Hurricane Nature Run as inspiration for the spatial pattern and daily variability of heating, we applied this to an idealized linear model, 3DVPAS, to explore the transition between balanced and radiating responses. The approach used in this study aims to test the mechanism in Dunion et al. (2014) for the origin of diurnal signals in the cirrus canopy, where radiative cooling of the cloud tops induces motion at sunset by modifying the local lapse rate.

Moist convective and radiative diurnal heating in the eyewall produce a balanced response in 3DVPAS, whereby the w' response is confined to the region near the source by the high inertial stability. Radiative diurnal heating in the cirrus canopy produces a radiating response throughout the depth of the cyclone, since the source of the heating/motion is in a region of lower inertial stability, as with the region in to which the waves are propagating. Waves produced by radiative heating of the cirrus canopy have predominantly diurnal and semi-diurnal frequencies, owing to the sharp inflection points in the radiative heating diurnal cycle. The results presented here suggest that diurnal signals beyond the inner core of a TC originate as a result of diurnal forcing of the cirrus canopy rather than the eyewall.

This work raises interesting questions about the impact of waves radiating from the cirrus canopy. For example, would any changes in intensity or structure result? To what extent can the forced lifting induced by wave radiation enhance convection or precipitation? Future work on this topic aims to address these questions in idealized models with nonlinear physics and additional hurricane simulations. Since this problem includes cloud physics, it is inherently nonlinear, and so future work should address this same problem in a non-linear framework.

Acknowledgements

This research was supported by the National Science Foundation under award AGS-1654831.

References

Dunion, J. P., C. D. Thorncroft, and C. S. Velden (2014). "The Tropical Cyclone Diurnal Cycle of Mature Hurricanes". In: *Monthly Weather Review* 142.10, pp. 3900–3919. URL: https://doi.org/10.1175/MWR-D-13-00191.1.

Gray, W. M. and R. W. Jacobson (1977). "Diurnal Variation of Deep Cumulus Convection". In: *Monthly Weather Review* 105.9, pp. 1171–1188. URL: https://doi.org/10.1175/1520-0493(1977)105%3C1171:DVODCC%3E2.0.CO;2.

Hodyss, D. and D. S. Nolan (2007). "Linear Anelastic Equations for Atmospheric Vortices". In: *Journal of the Atmospheric Sciences* 64.8, pp. 2947–2959. URL: https://doi.org/10.1175/JAS3991.1.

Iacono, M. J., J. S. Delamere, E. J. Mlawer, M. W. Shephard, S. A. Clough, and W. D. Collins (2008). "Radiative Forcing by Long-Lived Greenhouse Gases: Calculations with the AER Radiative Transfer Models". In: *Journal of Geophysical Research: Atmospheres* 113.D13. URL: https://agupubs.onlinelibrary.wiley.com/doi/abs/10.1029/2008JD009944.

Kossin, J. P. (2002). "Daily Hurricane Variability Inferred from GOES Infrared Imagery". In: *Monthly Weather Review* 130.9, pp. 2260–2270. URL: https://doi.org/10.1175/1520-0493(2002)130%3C2260:DHVIFG%3E2.0.CO;2.

Mecikalski, J. R. and G. J. Tripoli (1998). "Inertial Available Kinetic Energy and the Dynamics of Tropical Plume Formation". In: *Monthly Weather Review* 126, pp. 2200–2216.

Navarro, E. L. and G. J. Hakim (2016). "Idealized Numerical Modeling of the Diurnal Cycle of Tropical Cyclones". In: *Journal of the Atmospheric Sciences* 73.10, pp. 4189–4201. URL: https://doi.org/10.1175/JAS-D-15-0349.1.

Navarro, E. L., G. J. Hakim, and H. E. Willoughby (2017). "Balanced Response of an Axisymmetric Tropical Cyclone to Periodic Diurnal Heating". In: *Journal of the Atmospheric Sciences* 74.10, pp. 3325–3337. URL: https://doi.org/10.1175/JAS-D-16-0279.1.

Nolan, D. S., R. Atlas, K. T. Bhatia, and L. R. Bucci (2013). "Development and validation of a hurricane nature run using the joint OSSE nature run and the WRF model". In: *Journal of Advances in Modeling Earth Systems* 5.2, pp. 382–405. URL: https://agupubs.onlinelibrary.wiley.com/doi/abs/10.1002/jame.20031.

Nolan, D. S., Y. Moon, and D. P. Stern (2007). "Tropical Cyclone Intensification from Asymmetric Convection: Energetics and Efficiency". In: *Journal of the Atmospheric Sciences* 64.10, pp. 3377–3405. URL: https://doi.org/10.1175/JAS3988.1.

O'Neill, M. E., D. Perez-Betancourt, and A. A. Wing (2017). "Accessible Environments for Diurnal-Period Waves in Simulated Tropical Cyclones". In: *Journal of the Atmospheric Sciences* 74.8, pp. 2489–2502. URL: https://doi.org/10.1175/JAS-D-16-0294.1.

Tang, X., Z.-M. Tan, J. Fang, Y. Q. Sun, and F. Zhang (2017). "Impact of the Diurnal Radiation Cycle on Secondary Eyewall Formation". In: *Journal of the Atmospheric Sciences* 74.9, pp. 3079–3098. URL: https://doi.org/10.1175/JAS-D-17-0020.1.

Tang, X. and F. Zhang (2016). "Impacts of the Diurnal Radiation Cycle on the Formation, Intensity, and Structure of Hurricane Edouard (2014)". In: *Journal of the Atmospheric Sciences* 73.7, pp. 2871–2892. URL: https://doi.org/10.1175/JAS-D-15-0283.1.

Willoughby, H. E. (2009). "Diabatically Induced Secondary Flows in Tropical Cyclones. Part II: Periodic Forcing". In: *Monthly Weather Review* 137.3, pp. 822–835. URL: https://doi.org/10.1175/2008MWR2658.1.